

Mechanism of the Sensitivity Enhancement in TiO₂ Hollow-Hemisphere Gas Sensors

Hi Gyu Moon,^{1,2} Ho Won Jang,^{1,*} Jin-Sang Kim,¹ Hyung-Ho Park,² and Seok-Jin Yoon^{1,*}

¹Electronic Materials Center, Korea Institute of Science and Technology (KIST), Seoul 136-791, Korea

²Department of Material science and Engineering, Yonsei University, Seoul 120-749, Korea

We investigate the mechanism of the sensitivity enhancement in TiO₂ hollow-hemisphere gas sensors. Using monolayer close-packed polystyrene microspheres as a sacrificial template, a TiO₂ thin film based on a network of ordered hollow hemispheres is formed by room-temperature sputtering deposition and subsequent calcination at 550°C. A thin film gas sensor based on the TiO₂ hollow hemispheres exhibits a 225% change in its resistance when exposed to 50 ppm CO at 250°C, whereas a gas sensor based on a flat TiO₂ film shows an 85% change. Numerical analysis reveals that the enhancement of the gas sensitivity in the hollow-hemisphere gas sensor is simply the result of an increase in the effective surface area for the adsorption of gas molecules.

Keywords: gas sensors, TiO₂, hollow hemispheres, effective surface area, CO

1. INTRODUCTION

Nanostructured or porous metal-oxide thin films are of great interest for applications to small, highly sensitive gas sensors with fast response times owing to the high surface-to-volume ratios of these films and their compatibility with well-established semiconductor processes.^[1,2] Various methods, such as pulsed laser deposition, wet solution processing, sol-gel processing, photolithographic patterning, glancing angle deposition, anodic oxidation, and anodized aluminum oxide templating have been demonstrated for the fabrication of nanostructured metal-oxide thin-film gas sensors. Enhanced gas performance of nanostructured metal oxide thin films obtained using colloidal templating,^[3,4] which is an effective means of fabricating quasi-ordered submicron hollow structures of various metal oxides,^[5,6] was recently reported.^[5,6] Hollow-hemisphere films of SnO₂ and TiO₂ metal oxides exhibited 200% to 400% higher gas sensitivity levels than their counterparts in flat films.^[3,4,7] However, such an enhancement falls short of the efficient detection of various gases possible with metal oxide sensor arrays.^[8] To improve the gas sensing properties of the hollow-hemispheres films further, the exact mechanism of the higher sensitivity of hollow-hemisphere metal oxide films relative to flat films should be understood; however, this remains unclear.

In this work, we investigate the mechanism of the higher sensitivity of hollow-hemisphere TiO₂ films compared to flat films. Using the monolayer colloid template, we obtain TiO₂

thin films composed of hollow hemispheres by room-temperature sputtering and calcination at 550°C. A gas sensor based on the TiO₂ hollow hemispheres exhibits enhanced CO gas sensing in comparison to a sensor based on a flat TiO₂ thin film. By a direct comparison between the sensitivity enhancement and the enlargement of the surface area, the mechanism of the higher sensitivity of the hollow-hemisphere TiO₂ films is revealed.

2. EXPERIMENTAL DETAILS

An aqueous suspension of 1 μm polystyrene spheres (2.6 wt. %, Polysciences) was used in this work to fabricate the colloid templates. The suspension was ultrasonicated for 3 hours to disperse the microspheres uniformly without agglomeration. SiO₂ (300 nm)/Si substrates were cleaned by rinsing in acetone, isopropyl alcohol, and deionized water in sequence. After preparing the substrates, a drop of the suspension was pipette-dripped onto a predefined region by an adhesive plastic mask on a substrate. To obtain the monolayer deposition of the spheres, the samples were spun by a spin coater at a speed of 1400 rpm. They were then dried for 6 h in a dry box at room temperature. The surface morphology of the samples was investigated using a scanning electron microscope (SEM) (XL-30 FEG-ESEM, Philips) operating at 15 kV.

After obtaining the colloidal templates, 100-nm-thick TiO₂ film was deposited onto the colloid-templated samples at room temperature by RF sputtering using a polycrystalline TiO₂ target. By varying the film thickness, it was found that 100 nm is the optimum thickness to obtain the highest sensi-

*Corresponding author: hwjang@kist.re.kr; sjyoon@kist.re.kr

tivity from the fabricated TiO₂ films. The base pressure, working pressure, RF power, gas flow rate, and growth rate were 2×10^{-6} mTorr, 10 mTorr, 150 W, 30 sccm Ar, and 6.3 nm/min, respectively. After the deposition of the film, the adhesive plastic masks on the samples were removed. The samples were then calcined in air at 550°C for 60 min to burn out the polymer microspheres and simultaneously improve the crystallinity of the TiO₂ films, resulting in igloo-like hollow hemispheres on the substrates. When the ramp-up speed of the temperature during the calcination process was reduced to 5°C/min, no change was found in the shapes of the hemispheres before and after the calcination procedure. The crystallinity of the TiO₂ thin films was characterized by a x-ray diffractometer, revealing that the as-deposited amorphous films were fully crystallized to polycrystalline anatase TiO₂ after calcination at 550°C.^[7]

In the same manner, TiO₂ hollow-hemisphere gas sensors were fabricated using SiO₂/Si substrates with Ptinterdigitated electrodes (IDEs) in which the gap between each electrode was 5 μm. For comparison, a gas sensor based on flat TiO₂ thin film was also fabricated. The responses of the TiO₂ hollow-hemisphere gas sensors to CO gas were measured at ~250°C and compared with that of flat TiO₂ thin film gas sensors. The dynamic responses of the gas sensors to CO were monitored while changing the flow gas from dry air to 1 ppm, 5 ppm, and 50 ppm CO mixed with dry air. To eliminate any interfering effect, we used a constant flow rate of 300 sccm for the dry air and the test gases. The sensor resistance was measured under a DC bias voltage of 1 V using a source measurement unit (Keithley 236).

3. RESULTS AND DISCUSSION

Figure 1(a) show a top-view SEM micrograph of a colloid template of polystyrene spheres on a SiO₂/Si substrate. Over an area of 0.5 mm², the colloidal template consists of the close-packed microspheres. It is clear that the template is a perfect monolayer of spheres, as shown in Fig. 1(b). In the multiple tests, an area of at least 2 mm × 3 mm was obtained without sphere-free regions, agglomerates, or nonuniform

multilayers. Using such a perfect colloid template, we fabricated TiO₂ hollow-hemisphere films, as shown in Fig. 2. From the top-view SEM image in Fig. 2(a), the shape of each hollow cell closely resembles a hexagon rather than a circle, as highlighted by the dotted line. Straighter lines are found near the faces in contact with neighboring cells. The cross-sectional view shown in Fig. 2(b) clearly shows that the resultant hollow units are nearly hemispherical rather than full spheres. This is explained by the sequence of events in which TiO₂ film is deposited on only the upper parts of the microspheres during the RF sputtering process while the film sits on the substrate gradually during the calcination process, resulting in the aforementioned igloo-like hollow structure. For this reason, the heights of the hollow hemispheres are lower than 1 μm (0.5 - 0.7 μm). Moreover, they are not as perfectly uniform as those of the original microspheres, as shown in Fig. 2(b). The cross-sectional micrograph shows holes near the bottoms of the hollow cells. These holes originate from the contact faces in the original template because the film is not deposited in the contact faces. Figure 2(c) shows a 50°-tilt-view of the hollow hemispheres on the substrate. This figure shows that no holes exist in the sample. In reality, each cell is connected to its neighbors with open channels (locations highlighted by arrows). When the sample was cut for the cross-sectional image, the channels were opened, resulting in the holes shown in Fig. 2(b).

The feasibility of the TiO₂ hollow hemispheres for gas sensor applications was assessed. Figure 3(a) shows an optical photograph of the fabricated TiO₂ gas sensor and a SEM micrograph of TiO₂ hollow hemispheres on the Pt-IDE-pattern substrate. Closed-packed TiO₂ hollow spheres are well formed on both the SiO₂/Si and Pt surfaces. The dynamic response curve of the TiO₂ hollow-hemisphere gas sensor to CO at 250°C is shown in Fig. 3(b). For comparison, that of a gas sensor based on a flat TiO₂ film is also plotted. With CO gases on and off, the two sensors exhibit quick response and recovery in the sensor resistances. It is interesting that the two sensors show nearly equal responses and recovery times, indicating identical mechanisms for the adsorption

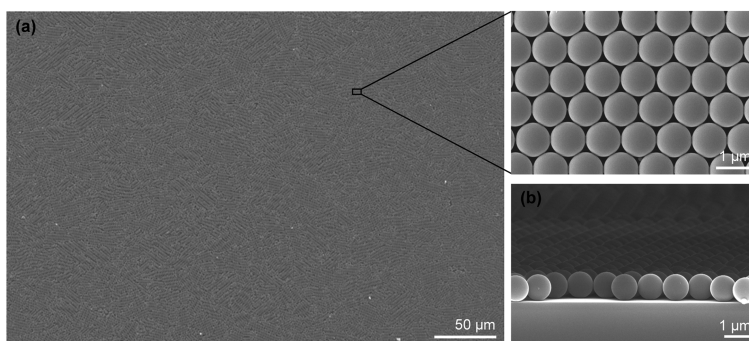


Fig. 1. (a) Top-view and (b) cross-sectional SEM micrographs of a large-area colloid template of monolayer microspheres on a SiO₂/Si substrate.

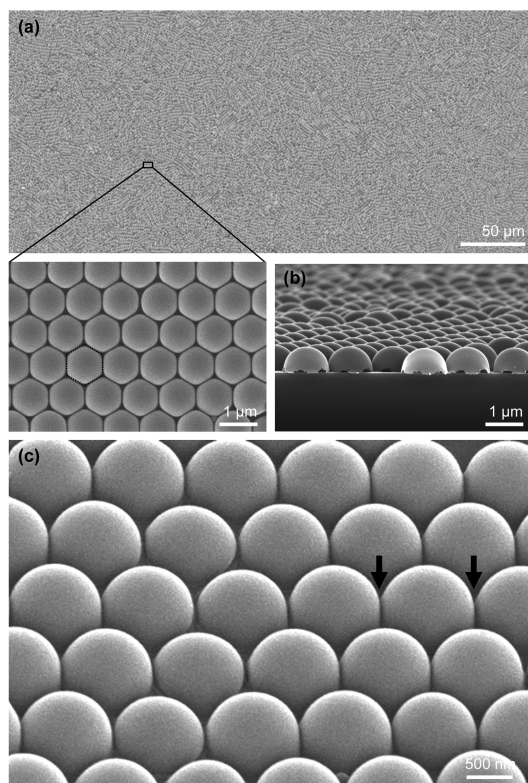


Fig. 2. (a) Top-view, (b) cross-sectional, and (c) 50°-tilt-view SEM micrographs of TiO₂ hollow hemispheres on a SiO₂/Si substrate. The arrows in (c) indicate links in which the hollow hemisphere is connected to the adjacent links without openings to ambient.

and desorption of gas molecules on the TiO₂ surface in both sensors. Figure 3(c) shows that the response and recovery time, defined as the time to reach 90% of the total resistance change, are 8 s and 40 s, respectively. These values are much smaller than previously reported values of TiO₂ gas sensors.^[9-14] In particular, the response time of 8 s is the fastest among all reported values for various semiconducting metal-oxide gas sensors.^[8] This is attributed to the narrow interdistance of 5 μm between the Pt IDEs.

The TiO₂ hollow-hemisphere sensor displays greater modulation of its sensor resistance than the flat-film sensor. To clarify this difference, the response of the R_{air}/R_{gas} ratio was plotted, as shown in Fig. 4, along with the response values of previously reported gas sensors based on nanocrystalline or nanosized TiO₂.^[7-9] For 50 ppm of CO gas, the response was found to be 1.85 and 3.2 for the flat-film and the hollow-hemisphere sensors, respectively. The enhancement of the response in the hollow-hemisphere sensor is consistent with the findings of previous reports.^[3,4] The response of 3.2 to 50 ppm of CO is comparable to or higher than the response times of nanostructured TiO₂ gas sensors.^[9-11] The CO detection limit for the hollow-hemisphere sensor was determined to be ~300 ppb, as indicated by the dashed line. It is interesting that the detection limit is nearly identical to that of the

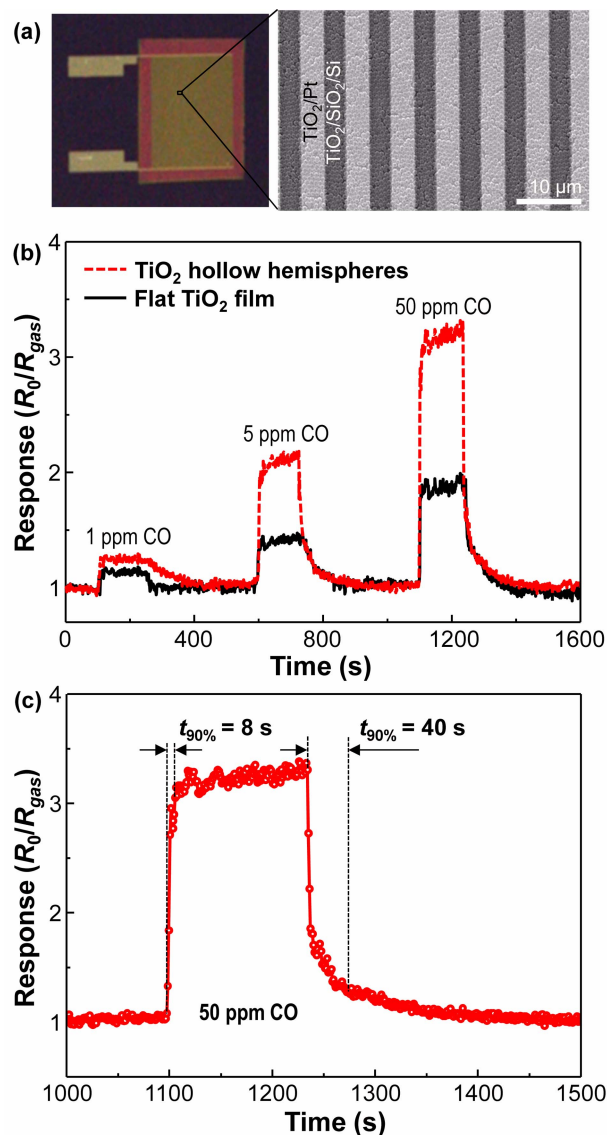


Fig. 3. (a) Photographs and SEM micrographs for a TiO₂ hollow-hemisphere gas sensor with a Pt IDEs. (b) Dynamic response curves of TiO₂ gas sensors based on a flat film and hollow hemispheres to 1–50 ppm CO gases at 250°C. The dashed line is a linear extrapolation to the curve of the TiO₂ hollow-hemisphere sensor. (c) Response time and recovery time of the TiO₂ hollow-hemisphere sensor to 50 ppm CO.

plain film. This result suggests that the detection limit cannot be improved merely by enlarging the surface area. It should be noted that the grain size of the TiO₂ hollow spheres was identical to that of the plain TiO₂ film.^[7,15] Consequently, the high sensitivity and the fast response time at the relatively low operation temperature of 250°C strongly suggest that the TiO₂ hollow-hemisphere gas sensor fabricated by large-area colloidal templating is highly suitable as a novel thin film gas sensor.

These findings strongly suggest that the increased surface-to-volume ratio of the hollow-hemisphere structure contrib-

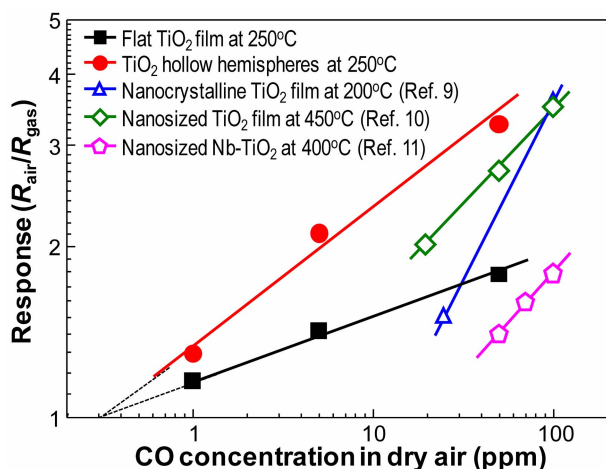


Fig. 4. Response of the TiO₂ hollow-hemisphere and flat TiO₂ gas sensors as a function of CO concentration in comparison with those of previously reported gas sensors based on nanostructured TiO₂.

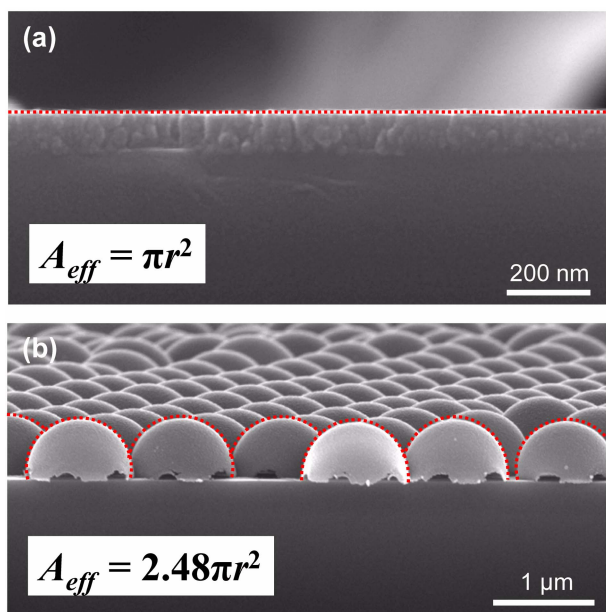


Fig. 5. Effective surface area for the adsorption of gas molecules, A_{eff} , for (a) the flat TiO₂ film and (b) the TiO₂ hollow hemispheres. The dot lines are guides to an eye for the effective surface area.

utes to the enhancement of the sensitivity. The effective surface area for the adsorption of gas molecules is calculated, as shown in Fig. 5 together with cross-sectional SEM micrographs. On a circular SiO₂/Si substrate with a certain radius of r , the effective surface area, A_{eff} , of the flat TiO₂ film is simply πr^2 . For the hollow hemispheres, the A_{eff} value for the adsorption of gas molecules is only the outer walls of the hollow hemispheres. As the hollow hemispheres are well connected to each other and because the inner spaces are not open to ambient air, as marked in Fig. 2(c), gas molecules cannot access the inner spaces of the hollow hemispheres.

Thus, the A_{eff} value for the hollow hemispheres was calculated to be $2.48 \pi r^2$ on average, which is between $4 \pi r^2$ for a full sphere and $2 \pi r^2$ for a hemisphere. It was also found that the surface area ratio, 2.48, is very close to the sensitivity ratio of 2.59 [= (3.21)/(1.851)], revealing that the enhancement of the gas sensitivity in the hollow-hemisphere gas sensor is due to the increase in the effective surface area for the adsorption of gas molecules. This result indicates that a further improvement in the gas sensitivity of the hollow-hemisphere gas sensor can be achieved by making the inner spaces active sites for the adsorption of gas molecules through the fabrication of open channels between the ambient air and the inner spaces of the hollow spheres. This is a focus of future work by the authors.^[16]

4. CONCLUSION

We have demonstrated the enhanced gas sensing properties of a TiO₂ hollow-hemisphere gas sensor fabricated using a colloidal template. The enhanced sensitivity of the sensor is attributed to the increase of the surface area for gas adsorption. Furthermore, it was suggested that a further improvement of gas sensing performance of the hollow-hemisphere sensor is possible via modification of the structure. We believe that TiO₂ hollow hemispheres are promising materials for various applications, such as air quality monitoring systems, environmental monitoring systems, ubiquitous sensor networks, and one-chip electronic noses.

ACKNOWLEDGMENT

The authors thank Beom-Keun Yoo, Min-Gyu Kang, and Young-Soek Shim for SEM measurements. This work was financially supported by the Core Technology of Materials Research and Development Program of the Korea Ministry of Intelligence and Economy (No. K0004114).

REFERENCES

1. Y. G. Choi, G. Sakai, K. Shimanoe, and N. Yamazoe, *Sens. Actuators B* **101**, 107 (2004).
2. M. W. Park and K. Y. Chun, *Electron. Mater. Lett.* **5**, 7 (2009).
3. I. D. Kim, A. Rothschild, D. J. Yang, and H. L. Tuller, *Sens. Actuators B* **130**, 9 (2008).
4. Y. E. Chang, D. Y. Youn, G. Ankonina, D. J. Yang, H. G. Kim, A. Rothschild, and I. D. Kim, *Chem. Commun.* 4019 (2009).
5. F. Caruso, R. A. Caruso, and H. Möhwald, *Science* **282**, 1111 (1998).
6. C. J. Martinez, B. Hockey, C. B. Montgomery, and S. Semancik, *Langmuir* **21**, 7937 (2005).
7. H. G. Moon, H. W. Jang, J. S. Kim, H. H. Park, and S. J.

- Yoon, *Electron. Mater. Lett.* **6**, 31 (2010).
8. G. Eranna, B. C. Joshi, D. P. Runthala, and R. P. Gupta, *Crit. Rev. Solid State Mater. Sci.* **29**, 111 (2004).
 9. M. R. Mohammadi, D. J. Fray, and M. Ghorbani, *Solid State Sci.* **10**, 884 (2008).
 10. V. Guidi, M. C. Carotta, M. Ferroni, G. Martinelli, L. Paglialonga, E. Comini, and G. Sberveglieri, *Sens. Actuators B* **57**, 197 (1999).
 11. A. Ruiz, A. Calleja, F. Espiell, A. Cornet, and J. R. Morante, *IEEE Sens. J.* **3**, 189 (2003).
 12. Z. Seeley, Y. J. Choi, and S. Bose, *Sens. Actuat. B* **140**, 98 (2009).
 13. M. R. Mohammadi, D. J. Fray, and M. C. Cordero-Cabrera, *Sens. Actuat. B* **124**, 74 (2007).
 14. M. H. Seo, M. Yuasa, T. Kida, J. S. Huh, K. Shimanoe, and N. Yamazoe, *Sens. Actuators B* **137**, 513 (2009).
 15. H. G. Moon, Y. S. Shim, H. W. Jang, J. S. Kim, K. J. Choi, C. Y. Kang, J. W. Choi, H. H. Park, and S. J. Yoon, *Sens. Actuat. B* **149**, 116 (2010).
 16. H. G. Moon, H. W. Jang, J. S. Kim, H. H. Park, and S. J. Yoon, *Sens. Actuat. B*, doi:10.1016/j.snb.2010.10.003.